Distinct periods of fan aggradation and incision for tributary valleys of different sizes along the Bailong River, eastern margin of the Tibetan Plateau

Yajun Li[1], Xingmin Meng[1*], Thomas Stevens[2], Simon Armitage[3], Shiqiang Bian[4], Guan Chen[1], Jianhua He[4]

1 School of Earth Sciences, Lanzhou University, Lanzhou, 730000, China.

2 Department of Earth Sciences, Villavägan 16, Uppsala University, 75236 Uppsala, Sweden.

3 Center for Quaternary Research, Department of Geography, Royal Holloway University of London, Egham, Surrey, TW20 0EX, United Kingdom.

4 College of Earth and Environmental Sciences, Lanzhou University, Lanzhou, 730000, China.

Abstract

Understanding the mechanisms of fan incision/aggradation provides key insights into the dynamics of fan evolution and hazardous fan-forming processes. This paper focuses on the discrepancy in fan evolution for two nearby valleys of different catchment areas along the Bailong River. Specifically, we study fan evolution in the small-sized CJB valley (watershed area being 1.1 km^2) using sedimentary analyses and ^{14}C dating. Sedimentary logging of seven exposed profiles indicates that mudflows and debris flows are the primary fan-forming processes. Seven samples were taken from paleosols developed in mudflow sediments, and the humin fraction was extracted for ^{14}C dating. These ages constrain the fan aggradation period between 10 - 4.9 kyr BP, and then the incision period occurred after 4.9 kyr BP. As the mudflow sediments may contain organic matter from hillslope legacies, the fan aggradation period may lag behind the ^{14}C ages defined in this study. In both conditions, the time of fan incision/aggradation in CJB is younger than that of the GLP valley (watershed area being 20 km^2) where fan aggradation occurred in 21.7 - 7 ka and incision occurred afterward. The fan aggradation period defined by the ^{14}C ages is consistent with an alluvial fan of similar thickness in the southeastern Tibetan Plateau and two other fans along the Bailong River. This consistency may suggest a plausible climatic control on fan evolution for small-sized tributary valleys, while the inconsistency with the larger GLP valley may suggest different climate-response regimes for tributary valleys of different sizes. More research on similar types of alluvial fans and cross-validation of different dating methods is needed.

Key words:

Alluvial fan; Bailong River; Eastern Tibetan Plateau; Aggradation and incision.

1. Introduction

Aggradation and incision are two prominent behaviors for alluvial fans in tributary-junction settings (Harvey, 1996; 2002; Larson et al., 2015; Harvey et al., 2016; Mather et al., 2017; Li et al., 2018). The transition between these two regimes is associated with the critical stream power threshold, which is defined by the ratio of critical power (the power required to transport the sediment supplied from the feeder catchment) to the actual power of the transport system (Bull, 1979; Harvey, 2012). Changes in the threshold can be caused by intrinsic (Clarke et al., 2010; Coulthard et al., 2005; Mather and Stokes, 2018; Nicholas et al., 2009; Nicholas and Quine, 2007) and/or extrinsic (climate, tectonism and base level) factors (Geach et al., 2015; Harvey et al., 2016; Kar et al., 2014; Owen et al., 1997; Owen et al., 2014; Ritter et al., 1995; Singh et al., 2016; Spelz et al., 2008; Suresh et al., 2007; Viseras et al., 2003). Understanding the controlling factors for fan incision/aggradation can provide important insights into the trends and rates of fan dynamics (Cabré et al.; Harvey, 1996; Harvey, 2012; Mather et al., 2017), and risk management of hazardous fan-constructing processes such as debris flows/hyperconcentrated floods(Crosta and Frattini, 2004; de Scally et al., 2010; Khan et al., 2013; Santangelo et al., 2012; Stolle et al., 2015; Welsh and Davies, 2011). Unlike river terraces which usually are a function of a regional fluvial system (Bridgland and Westaway, 2014; Stokes et al., 2012), alluvial fans developed in tributary-junction settings may be shaped by tributary valleys with distinct characteristics (Mather et al., 2017; Stokes and

Mather, 2015). Consequently, fan-forming processes and controlling factors may be different for different tributary valleys. Deciphering the controlling factors for different types of alluvial fans can deepen our understanding of the variability of hillslope-river connectivity and the activities of hazardous processes (debris flows or floods).

This paper reports a case study of distinct fan aggradation and incision stages and controlling factors in two tributary valleys of the Bailong River, hence adding to the knowledge of complex responses of fan systems to external forcing. The Bailong River is on the margin of the eastern Tibetan Plateau, featuring high-relief steep hillslopes and deeply incised valleys (Li et al., 2018; Xiong et al., 2016). Under the influence of concentrated rainstorms during the summer, vast amounts of coarse sediments are transported from the tributary valleys, and deposited on the floodplains of the Bailong River, forming tributary-junction alluvial fans (Li et al, 2018). The tributary valleys of the Bailong River can be classified into large-sized (>100 km^2), mid-sized (10-100 km^2) and small-sized (< 10 km^2) categories according to watershed areas. In a previous study, we have studied the development of alluvial fans in the GLP valley, representing the mid-sized valleys of the Bailong River (Li et al., 2018). We identified four morphostratigraphically distinct, gently-sloping surfaces, denoted as F1, F2, F3, and F4 from the lowest to the highest fans in the GLP valley. Sedimentary analyses indicate that these alluvial fans were formed by debris flows and hyperconcentrated floods. Using OSL dating, the formation periods of the alluvial fans were constrained to before 90.0 ± 10.0 ka for F4, 21.7 ± 2.5 to 7.1 ± 0.7 ka for F3 and 1.4 ± 0.1 to 0.6 ± 0.1 ka for F2. By comparing the temporal correlations between fan formation and regional climatic records, a climatic control has been suggested to explain the evolution of the F4 and F3 alluvial fans in the GLP valley (Li et al., 2018). According to this model, a cold and/or dry climate caused an increased supply of sediment which led to fan aggradation during infrequent rainstorms and sediment-rich flows, while a warm and wet climate caused increased vegetation cover and frequencies of flood discharges, leading to fan incision. However, it is unknown whether this climate-fan response model developed for the mid-sized tributary valley equally applies to the small-sized valleys of the Bailong River. This question is important to answer to obtain a comprehensive understanding of the controlling factors for alluvial fans sourced from different valleys, as well as the risks for residents living on fan surfaces from future debris flows or floods. To answer the aforementioned question, the Chenjiaba (CJB) valley is chosen for study because it is close to and poses similar geological settings to the GLP valley. This paper first analyzes the topographic characteristics of the two valleys to denote the similarities and differences between the two valleys. We then use sedimentary logging to characterize and identify the constructing processes that formed the alluvial fans in the CJB valley. We take soil samples from the base and top of fan exposures for ^{14}C dating, and the ^{14}C ages are used to constrain the timing of fan aggradation and incision. The evolution periods and controlling factors in the two valleys are compared and discussed.

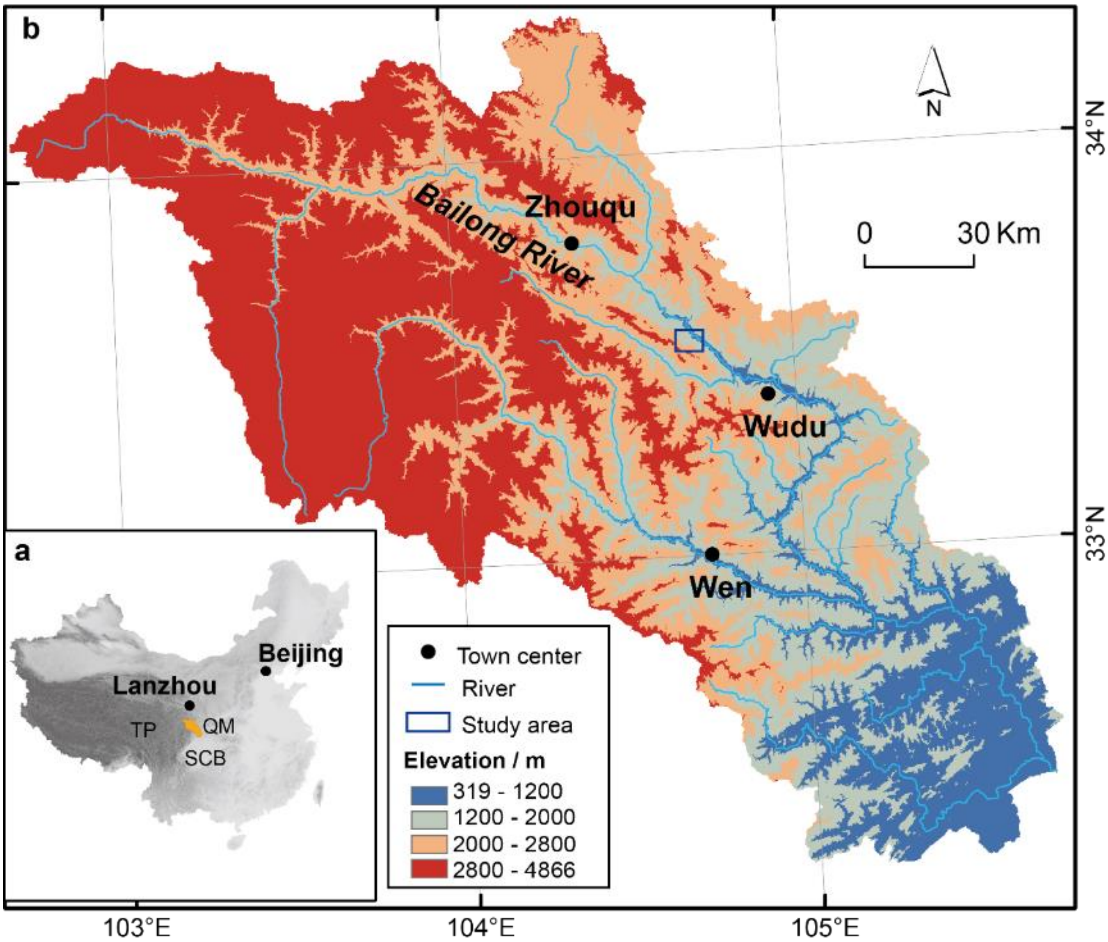

Fig. 1. Location of the Bailong River and the study area. (a) . Location of the Bailong River (the area shaded in orange) in China. TP=Tibetan Plateau; SCB=Sichuan Basin; QM=Qinling Mountain. (b). DEM of the watershed of the Bailong River and the location (blue rectangle) of the study area

2. Study area

The Bailong River lies in the transitional area of the Tibetan Plateau, the Western Qinling Mountains, and the Sichuan Basin (Fig. 1). The valleys studied here lie in the mid-section of the Bailong River, i.e., the section between Zhouqu and Wudu (Figs. 1&2). The geological strata in this section cover the Silurian to the Quaternary. The characteristic rocks are phyllites, limestones, and slates. Specifically, Silurian strata, with the primary lithology being phyllite or slate, are the major set of strata in the region, while the Devonian, Carboniferous, Permian, and Triassic, represented mostly by limestones, are distributed to the north and south of the Silurian strata (Fig. 2), forming an anticline structure. The Jurassic, Cretaceous, Paleogene, and Neogene strata are composed of sandstones and conglomerates which are only present in some local basins. The Quaternary strata, including a series of alluvial, colluvial, and aeolian deposits, are distributed along the banks of the Bailong River, in topographically low areas and flat hill-slopes. The mid-section of the Bailong River develops in Silurian phyllite bedrocks, which are confined by Carboniferous/Permian limestones to its north and south (Fig. 2). The relatively high-elevation limestone areas generally form the upper headwaters for most tributary valleys, while the relatively low-elevation phyllite area forms the lower part of the tributary valleys (Fig. 2).

There are 133 small-sized and 38 mid-sized tributary valleys in this section (Fig. 2). The mean slopes for the small-sized and mid-sized valleys are 28.9° and 29.1°, respectively, while the mean reliefs are 1070m and 1901 m, respectively. Here we select two nearby valleys, the GLP valley and the CJB valley as our study area (Fig. 2). The GLP valley (with a watershed area of 20 km^2) and the

CJB valley (with a watershed area of 1.1 km^2) represent the mid- and small-sized tributary valleys of the Bailong River, respectively (Fig. 2). These two types of valleys are the main valleys that develop alluvial fans along the Bailong River. The CJB valley develops in a similar geological setting to the GLP valley. The upper parts of these two valleys both develop in the high-elevation limestone area, while the lower parts develop in the low-elevation phyllite area (Fig. 2). The two valleys are both transected by a strike-slip thrust trending NW 70° (Fig. 2).

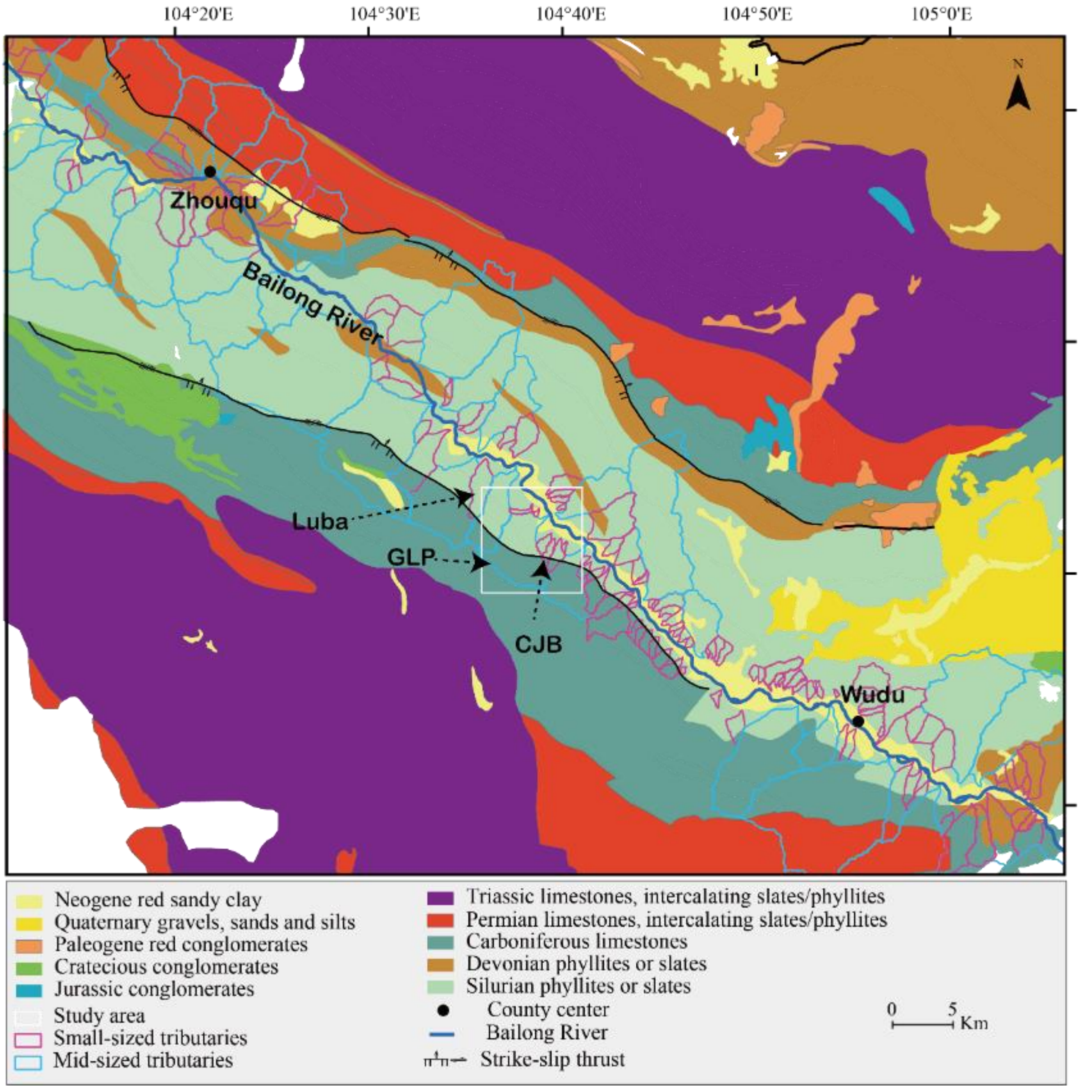

Fig. 2. Geology of the mid-section of the Bailong River. The white rectangle is where the GLP

and the CJB valleys reside.

Vegetation cover in the area can be classified into three zones. The high-elevation limestone areas are dominated by coniferous forests and shrubs (Fig. 3). Pinus is the major species, and some Quercus, Ulmus, and Betula are also present in the limestone area. The loess-covered phyllite hillslopes are mainly covered by grasses (Fig. 3) which include Poaceae, Zygophyllaceae, Compositae, Chenopodiaceae, Artemisa, Ranunculaceae, and Chenopodiaceae, etc. The alluvial fans and the floodplains of the Bailong River are mainly used for agricultural lands such as rapeseed, wheat, and corn. Some broad-leaved trees are also distributed in this area.

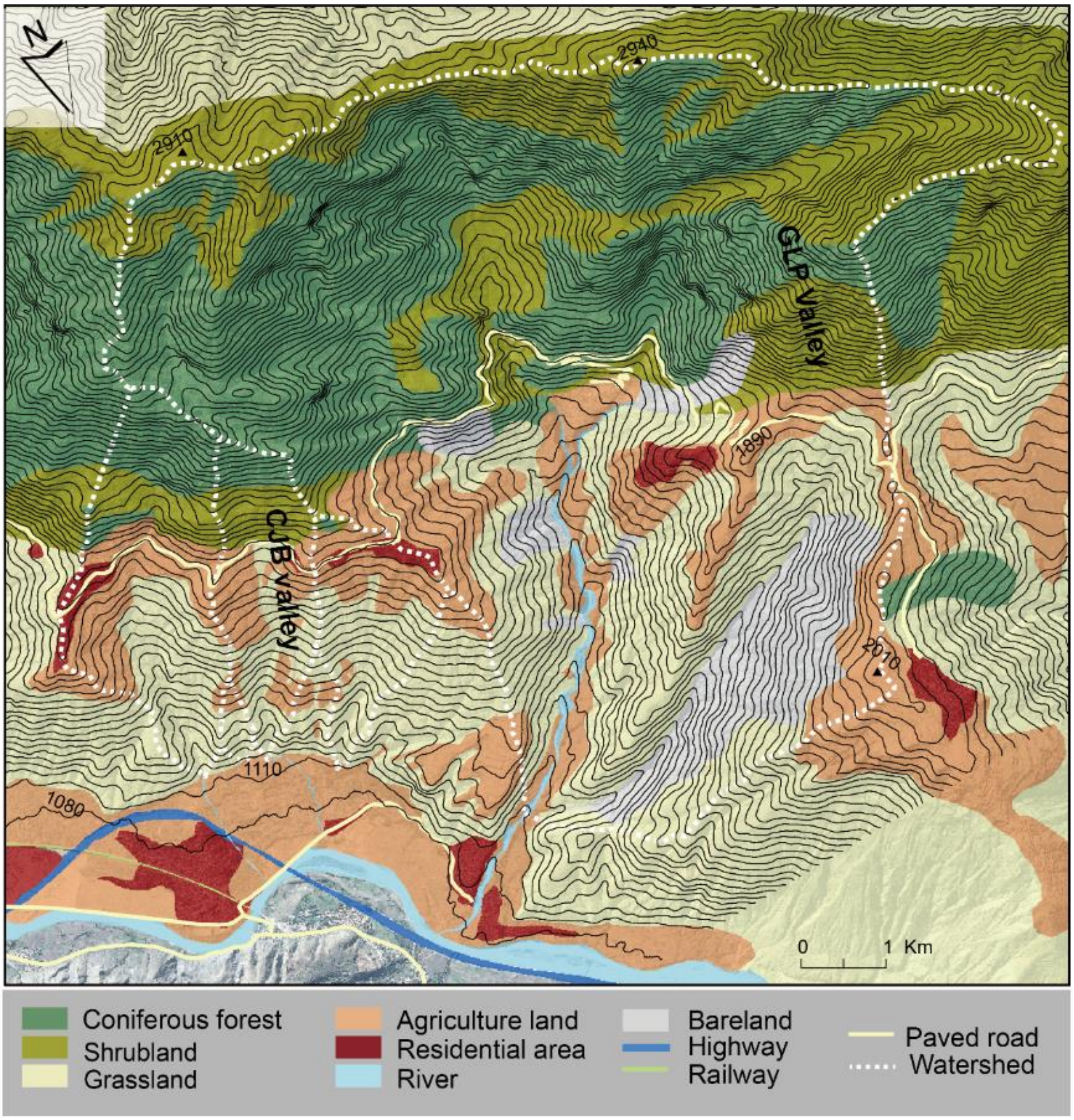

Fig.3 Map of land uses in the CJB and the GLP valleys. The elevation intervals of the contour lines are 30 m.

3. Methods

This study analyze the topographic characteristics of the two valleys based on a 30-m resolution ASTER DEM. The “Hydrology” toolbox of ArcGIS was used to derive the topographic features such as watershed area, relief, mean slopes and Strahler numbers etc. We then used methods of sedimentary logging to depict the nature of the processes that formed the alluvial fans in the CJB valley. Sedimentary logs were conducted for exposed outcrops of alluvial fans. Description features such as roundness, sorting, and bedding were recorded for each sedimentation unit. The grain size distribution was measured using sieving (for coarse sediments) and laser diffraction (for fine sediments). To detect the provenance of gravelly sediments, the clast lithologies are counted for the sieved gravels. The sedimentary units were annotated using the standard lithofacies codes (Miall, 2006), and the depositional processes were interpreted based on present knowledge of the sedimentary characteristics of different alluvial processes (Blair and Mcpherson, 1994; Dasgupta and Manna, 2011; Iverson, 1997).

^{14}C dating of paleosols is used to constrain the timing of alluvial fan aggradation and incision. Seven paleosol samples were taken from the fan exposures in the CJB valley. We used the humin fraction from soils for ^{14}C dating because this fraction is insoluble in aqueous solution, resulting in a relatively low probability of carbon contamination from overlying material (Inoue et al., 2011; Pessenda et al., 2001). It is noteworthy that the clay-sized humin fraction may be contaminated by reworked hillslope organic matter. Consequently, it is possible that this matter may provide older ages for paleosols. All samples were prepared with the standard pre-treatment (acid-alkali-acid) and then were converted to graphite in the Automated Grap hitization Equipment (AGE III).

AMS analyses were performed in a MICADAS system (MICADAS 20) of the Lanzhou University. Data reduction was performed with BATS, the computer program with the MICADAS, using OXAII standards and phthalic acid (C8H6O4) blanks for normalization and background correction. The ^{14}C results are expressed as a fraction of modern Carbon (14F) that represents the $^{14}C/^{12}C$ ratio of the sample related to the isotopic ratio in 1950. The ages reported are given in BP, years before present, where present is AD 1950. The IntCal13 curve was used to calibrate the dates, using the program OxCal4.3 (Bronk Ramsey, 2009).

4. Result

4.1 Topographic characteristics of the GLP and the CJB valleys

The topographic characteristics of the GLP and the CJB valleys are listed in Table 1, and the geomorphic settings of the two valleys are presented in Fig. 4. The topographic range is 1177 m for the CJB catchment and 1850 m for the GLP catchment. The mean slopes for the CJB valley and the GLP valley are 26.8° and 29.7°, respectively. The GLP valley develops high-order (Strahler number = 4) channels that deeply incise through the phyllite and limestone bedrocks. In contrast, the CJB valley develops low order (Strahler number = 2) channels in the loess-covered phyllite area. The percentages of loess area in the two valleys are different: loess accounts for 50% of the catchment area for the CJB valley, while it only accounts for 9% of the catchment area for the GLP valley. In the GLP valley, loess is mainly distributed on the divides of phyllite hillslope, while in the CJB valley, almost the whole phyllite hillslopes are covered by loess (Fig. 4). In both valleys, the limestone bedrock develops highly-fractured spaced joints that may be the sources for coarse and angular regolith and colluviums (Fig. 5a). Much of the loess on the hillslopes is either mixed or intercalated with limestone/phyllite gravels (Figs. 5b&4c) indicating the influence by hillslope processes during the deposition of loess. At some sections along the channels, phyllite bedrock is exposed with loess overlying the phyllite regolith.

Table 1 Topographic characteristics of the CJB and the GLP valleys.

	GLP	CJB
Catchment area	20	1.1
Topographic range	1850	1177
Mean slopes	29.7°	26.8°
Areal percentage of loess	9%	50%
Highest Strahler number	4	2

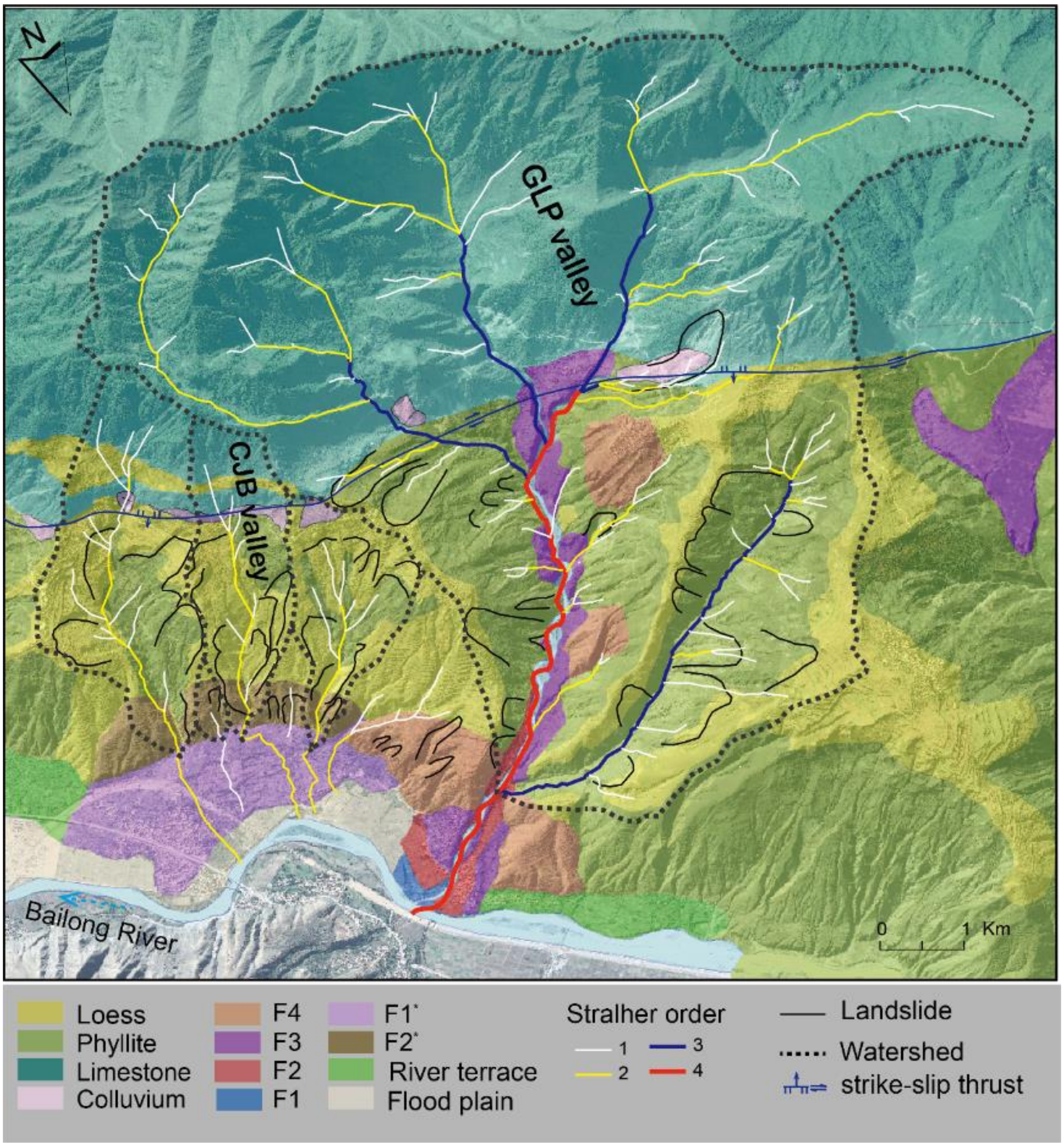

Fig. 4. Geomorphic setting of the GLP valley and the CJB valley. F1, F2, F3 and F4 represent the four levels of the alluvial fans of the GLP valley. F1* and F2* represents the low- and high-level alluvial fans formed by the CJB valley and the other two nearby valleys.

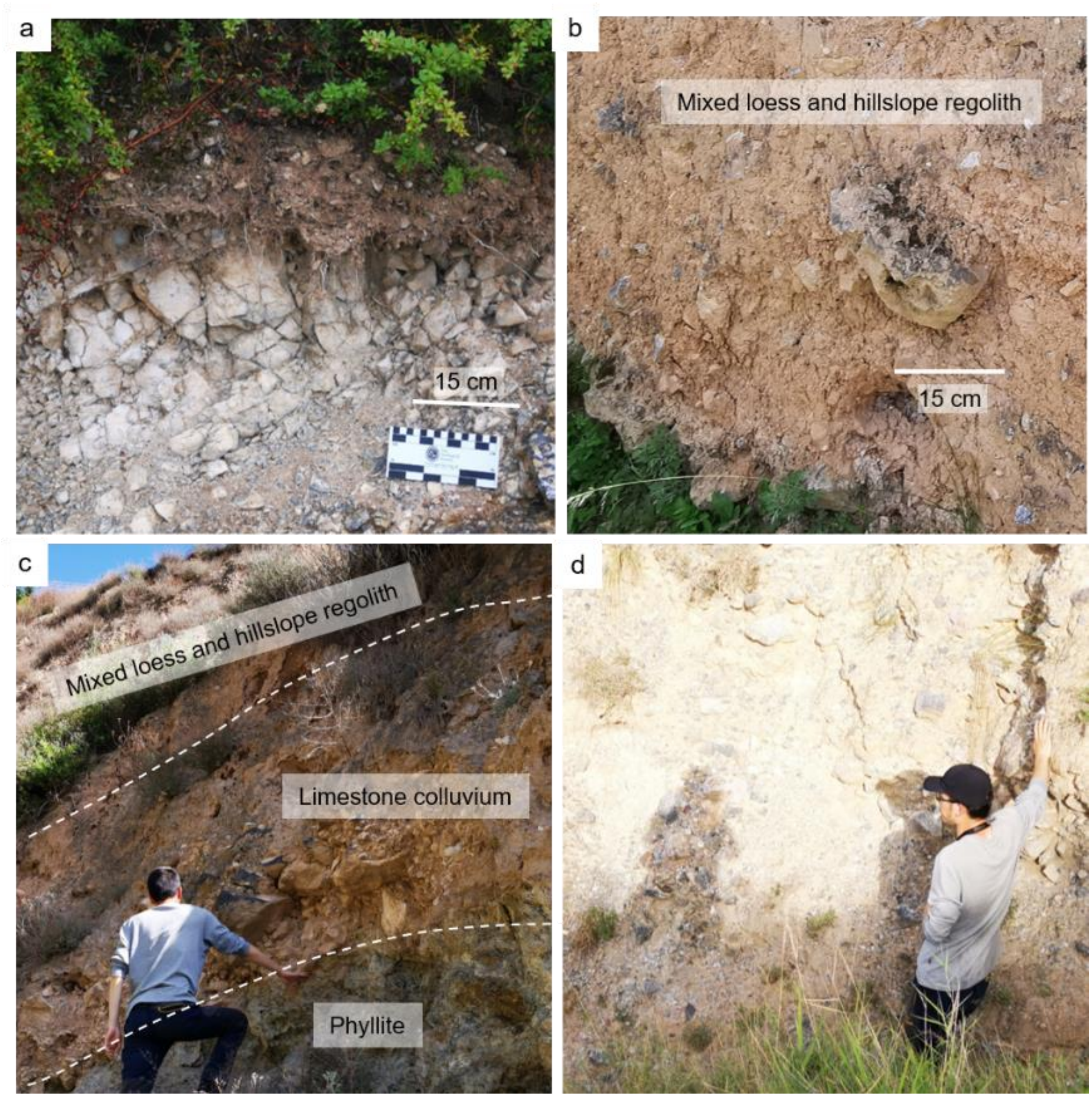

Fig. 5 Photographs of typical hillslope materials in the CJB valley. a. highly fractured limestone regolith which are covered by brush. b. mixed loess and limestone gravels. c. phyllite bedrock, limestone colluvium and mixed loess and gravels. d. limestone dominated alluvial sediments of the F2*.

In GLP, four morphostratigraphically distinct, gently-sloping surfaces are identified and denoted as F1, F2, F3, and F4 from the lowest to the highest fans (Figs. 4&6). The F1 alluvial fans are 5 m above the Bailong River (Fig. 6), and the F2 alluvial fans are ~10 m above the Bailong River. Both levels of alluvial fans have gentle surface grades (~ 2°) and are mainly distributed at the mouth of the GLP valley (Fig. 4). The surface of the F3 alluvial fans is ~ 50 m above the Bailong River with a surface grade of 5°, and the F3 alluvial fans are distributed along the main channels of the GLP valley (Fig. 4). The surface of the F4 alluvial fans is ~200 m above the Bailong River with a surface grade of 7°. In CJB, two prominent levels of alluvial fans exist. The high-level fan ($F2^{*}$) is at the same level of the F4 alluvial fans of the GLP valley (Fig. 6 & Table 2). Both the $F2^{*}$ and the F4 alluvial fans are composed of fluvial sediments (well-rounded gravels and sands) of the Bailong River, debris flow sediments of the local hillslopes (Fig. 5d) and loess. The low-level fan ($F1^{*}$) is ~25 m above the Bailong River with a surface grade of $\sim 10^{\circ}$. This level of alluvial fan combines the sediments from other nearby channels and forming a bajada (Fig. 4).

Table 2. Characteristics of different levels of alluvial fans in the GLP valley and the CJB valley. The surface slopes of alluvial fans in the GLP valley were measured based on a DEM obtained using a 3D laser scanner (Riegle LPM-321). The surface slopes in the CJB valley are measured based on the 30-m resolution ASTER DEM. H refers to the surface height above the Bailong River

Location	Fan level	Surface slope (°)	H (m)
GLP	F1	2	5
	F2	2	10

	F3	5	50
	F4	7	200
CJB	F1*	10	25
	F2*	15	200

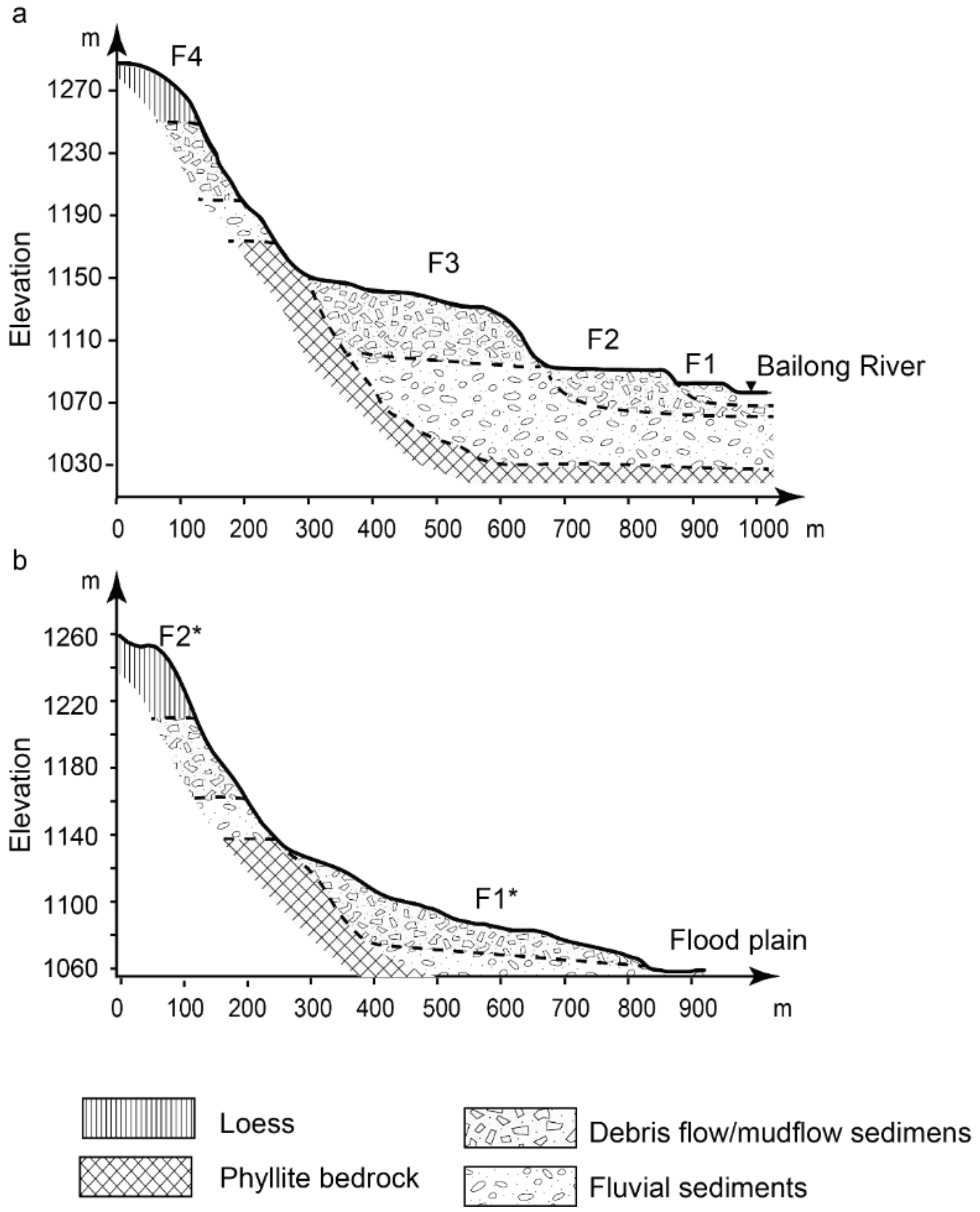

Fig. 6 Topographic transects illustrating the relative positions of the alluvial fans in GLP (panel a) and CJB (panel b). Dashed lines are estimated boundaries between different units.

4.2 Fan sedimentology

The sedimentology of alluvial fans in the GLP valley has been analyzed in Li et al (2018), and this paper mainly focuses on the alluvial fans in the CJB valley. We logged four fan exposures along the main channel and three exposures along the fan margin (Figs. 7&8) for the CJB valley. Sedimentary analyses reveal six types of lithofacies: Gci, Gcm, Gh, S, Fm, Fm'.

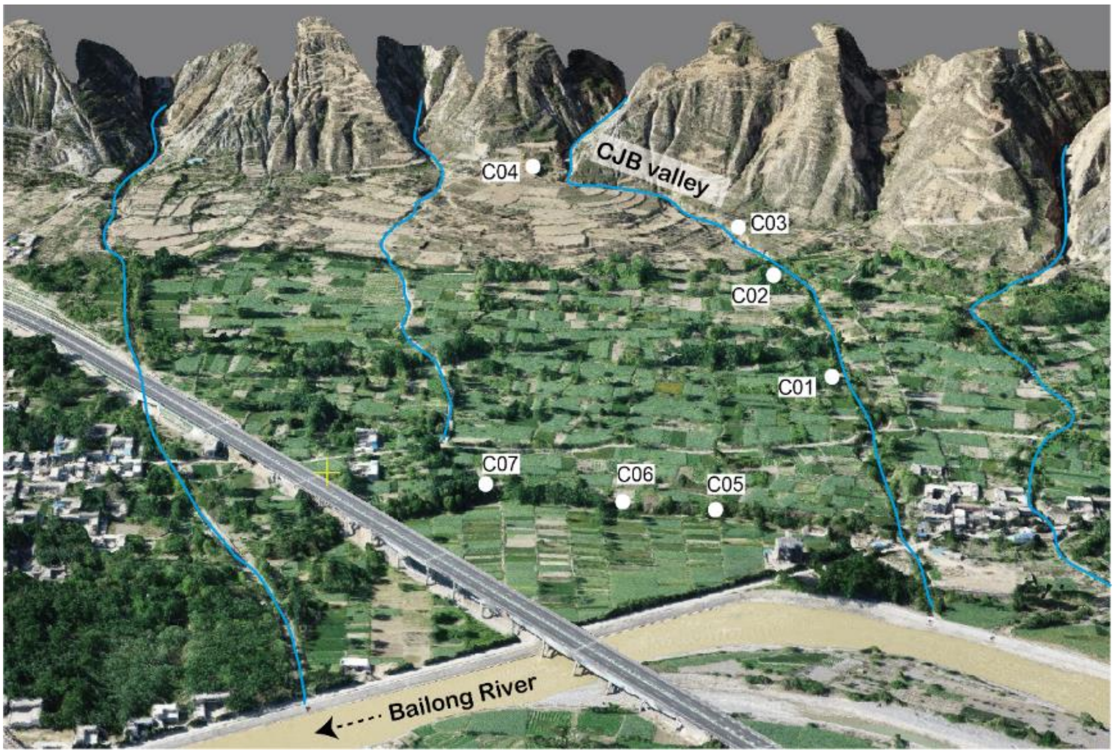

Fig. 7 Location of the profiles for sedimentary logging. The image is obtained using a drone (model: DJ Phantom 4 pro). The white dots are the locations of the sedimentary logs. The blue lines are the channels incised into the alluvial fans.

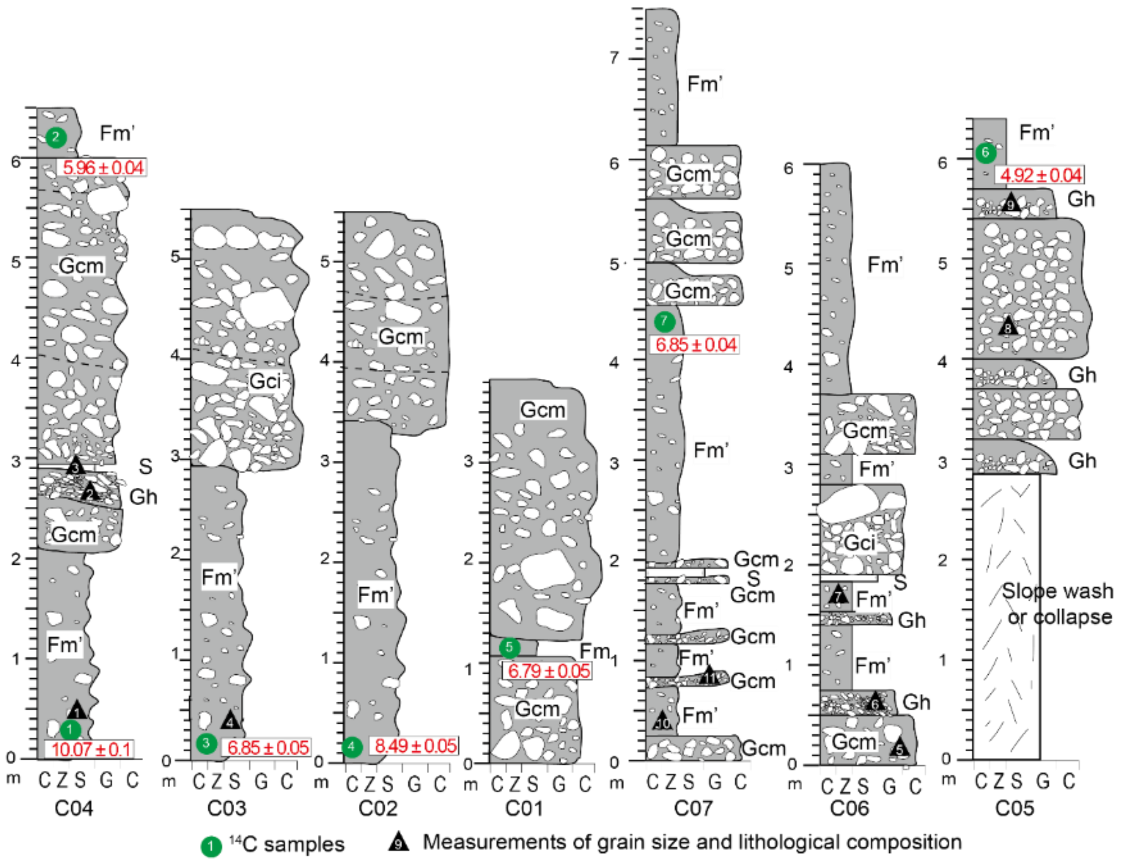

Fig. 8. Sedimentary logs and ^{14}C ages (kyr BP) in the CJB valley. The location of each log is presented in Fig. 7.

Lithofacies Gci and Gcm both refer to poorly sorted clast-supported cobble to pebble clasts (Figs. 9a&9b). Clasts are inversely graded in lithofacies Gci but show no obvious grading in lithofacies Gcm (Figs. 9a&9b). The bed thickness for both lithofacies is usually larger than 50 cm. Grain size analyses for three samples indicate that gravels (> 2 mm fractions) account for about 80% of the total sample weight, and sediments are poorly sorted (Fig. 10a). Limestone forms the primary clast lithology (> 60%) in the three samples, and phyllite accounts for 30-40% in the total counts (Fig. 11). The coarse poorly-sorted sediments indicate that lithofacies Gci & Gcm have been deposited by debris flows (Bagnold, 1954; Dasgupta and Manna, 2011; Iverson, 1997; Middleton, 1970; Pierson and Costa, 1987; Takahashi, 1981). These lithofacies are mainly present in the upper parts of the sedimentary profiles along the main channel, whereas they are also present on the lower portion of the exposures on the distal margin of the alluvial fans (Fig. 8).

Lithofacies Gh refers to poorly sorted, crudely bedded clast-supported sandy gravels (Fig. 9c). Individual beds are 10–20 cm thick, and the beds lack internal grading (Fig. 9c). Grain-size analyses for three samples show that the major fractions are very coarse sands (1- 2 mm diameter) to medium gravels (8 – 16 mm diameter) which together account for more than 60% of the sample weights (Fig. 10b). The proportion of limestone clasts is larger than that of phyllite clasts in two of the samples (samples 2 and 9), while in sample 6 phyllites form the major lithology (Fig. 11). The crude bedding in the sediments indicates that they have been deposited as a traction-carpet (Sohn, 1997), suggesting a process dominated by hyperconcentrated flows (Hungr et al., 2014; Went, 2005). These lithofacies usually account for a small proportion of each profile (Fig. 8).

Lithofacies Fm’ refers to sandy mud which is mixed with some gravels (Figs. 9d&9e). Gravels are generally dispersed in the mud (Fig. 9d). This lithofacies usually accounts for a major proportion of the exposed profiles (Fig. 8). For the fan exposures along the main channel, these lithofacies are mainly found in the lower part of exposures; while for the exposures along the fan margins, they are also present in the upper parts of the exposures (Fig. 8). Although dominated by fine materials, the proportion of gravels within the samples is variable (Figs. 9d&9e). According to the sieving results for four samples, the percentage of gravels within the sediments varies between 3-35% (Fig. 10c). The samples used for ^{14}C dating were taken from these sediments. These dated samples were also analyzed for grain size distribution (Fig. 10d). The results suggest that silt accounts for the major proportion of the sediment. Lithological compositions for the gravels in the four samples also vary in terms of the relative contents of limestone and phyllite clasts (Fig. 11). The lack of internal stratification, the poorly sorted nature of the fine sediments and the dispersed gravels in muds indicate that they were deposited by mudflows (Curry, 1966; Hungr et al., 2001; Ma et al., 2005; Wuji et al., 2016; Zha et al., 2019).

Lithofacies Fm refers to horizontally-laminated sandy mud (Fig. 9f). The fine materials form thin (10 - 20 cm) flat beds. One sample was taken for laser diffraction analysis, and the result suggests that the grain size distribution is similar to the Fm' sediments (Fig. 10d). This thin-layer of laminated sandy mud has been found on the top of many debris flow sediments in the Bailong River (Xiong and Cui, 1991). They have been interpreted as deposition by hyperconcentrated streamflows following debris flow deposition (Xiong and Cui, 1991). Hyperconcentrated streamflows are muddy streamflows with damped turbulence and are common processes in loess-covered areas (Qian and Wang, 1983). Hyperconcentrated streamflows usually develop a measurable yield strength (Pierson and Costa, 1987) such that their sediments are not very well-sorted compared to normal streamflows, but they can still form lamination by multiple surges. **Lithofacies S** refers to horizontally-bedded sands which are usually about 10 cm thick (Fig. 8). This lithofacies may be deposited by normal stream floods.

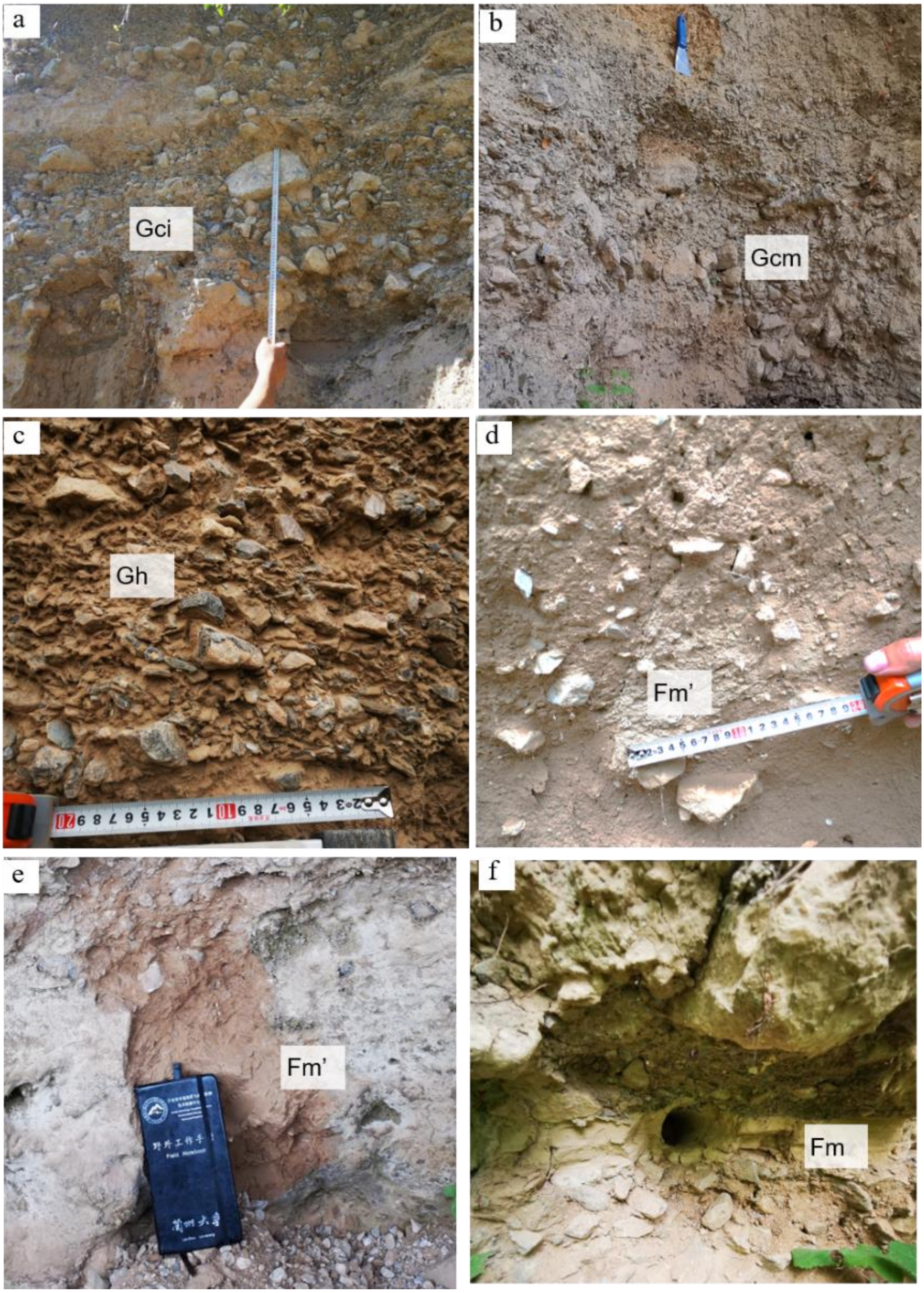

Fig. 9. Typical photographs of the lithofacies identified in the study.

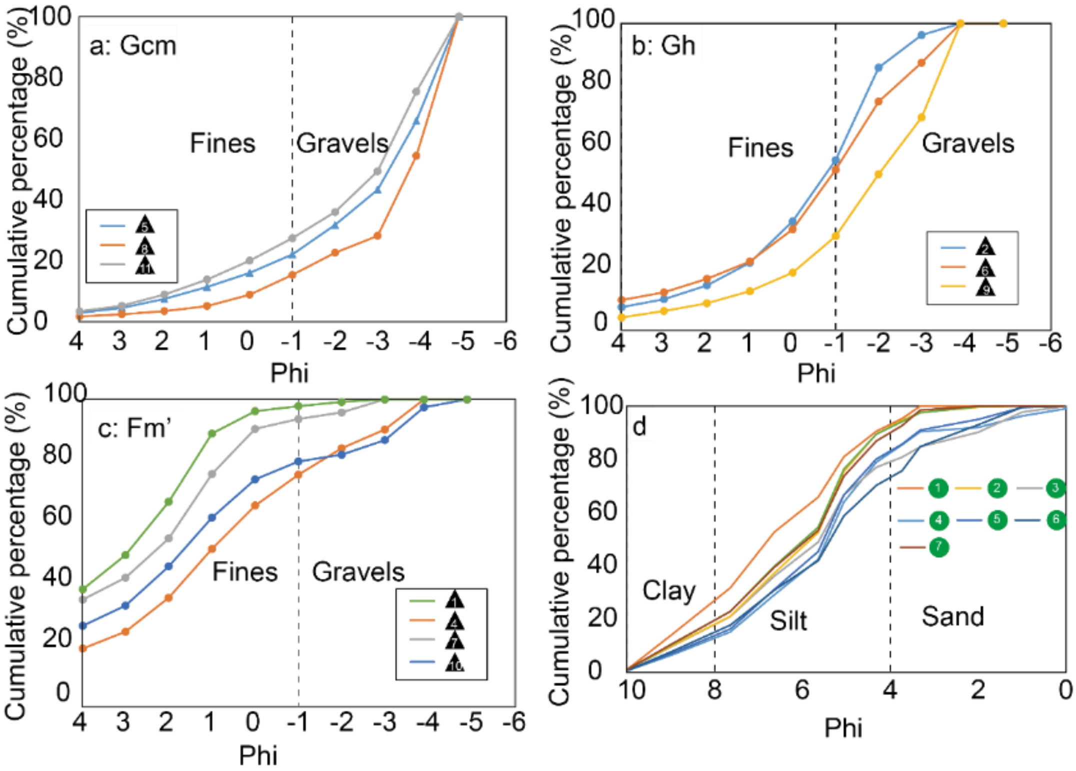

Fig. 10 Grain size distribution for different lithofacies. Panels a, b and c present the results of sieving, while panel d presents laser diffraction results for the samples used for ^{14}C dating.

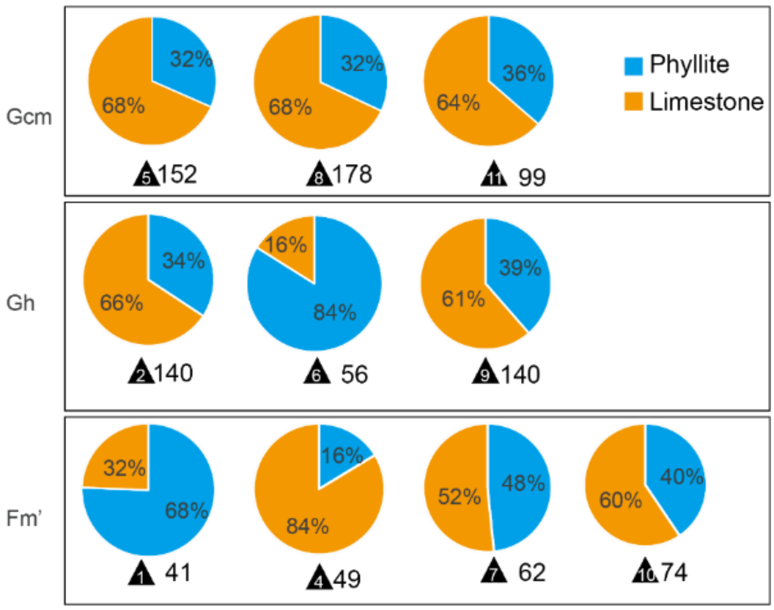

Fig. 11. Result of lithological composition. The numbered triangles represent sample codes denoted in Fig. 8. The numbers represent the total count of clasts.

4.3 Fan chronology

Six samples were taken from lithofacies Fm’ for ^{14}C dating in the CJB valley (Fig. 8). Specifically, the samples were taken from the Fm’ sediments where the fine fractions (< 2mm) account for more than 90% of the sample, and the sample color is reddish-brown. We consider that the color may suggest post-depositional pedogenesis processes developed in the sediment, though we cannot preclude the potential source from the original hillslopes. The dating result is presented in Table 3. The oldest age (10.07 ± 0.1 kyrs BP) is provided by sample 01, which was taken from the base of the proximal fan exposure (Fig. 8). Sample 02, which was taken from the top of the profile, produces an age of 5.96 ± 0.04 kyrs BP ka. These two ages fit the stratigraphic order. Three samples (samples 03, 04, and 07) which were taken from the lower portions of three separate profiles provide ages between 8.49 – 6.85 kyr BP. Sample 06, which was taken from the top of profile C05 (Fig. 8), provides the youngest age, 4.92 ± 0.04 kyr BP. Besides, we took one sample (sample 05) from lithofacies Fm and obtained an age of 6.79 ± 0.05 kyrs BP (Fig. 8). As we used the humin fraction within soils to measure the ^{14}C ages, potential contamination by younger materials such as invasion of roots and infiltration of organic compositions etc., is not possible. However, the clay-sized non-hydrolysable humin may be contaminated by the legacies of hillslope materials. Consequently, the ^{14}C ages reported in this study may be older estimates than the true time of the mudflow events.

Table 3 Radiocarbon dates of samples from the CJB valley. C (%) refers to the carbon contents of the samples that have been processed by the acid-alkali-acid treatment.

Code	Dating material	C (%)	$F^{14}C$ (pMC)	age (y)	Cal. Age (yr BP) 1σ
01	Humins	0.10	32.82±0.38	8950 ± 30	10074±124
02	Humins	0.25	52.28±0.36	5210±30	5960±39
03	Humins	0.10	47.27±0.26	6020±20	6847±48
04	Humins	0.10	38.32±0.34	7710±30	8493±45
05	Humins	0.12	47.60±0.27	5960 ± 20	6794±47
06	Humins	0.27	58.09±0.24	4360±20	4918±36
07	Humins	0.36	4.33±0.27	6010±30	6850±44

5. Discussion

5.1. Fan formation processes and valley development

According to the sedimentary analyses, the primary processes for the CJB alluvial fans are debris flows and mudflows. This is in contrast with the alluvial fans in the GLP valley where debris flows and hyperconcentrated floods are the primary processes with few mudflow sediments being identified (Li et al., 2018; Li, 2018). The areal extent of loess only accounts for 9% of the watershed area of the GLP valley, while it accounts for 50% of the watershed area of the CJB valley. It is inferred that the difference in loess distribution has determined the distinct fan-forming processes of the two valleys. As loess is generally stored on relatively less-steep hillslopes, the topographic conditions, specifically the hillslope gradients, may also contribute to the distinction of fan-forming processes in the two valleys.

The lithological composition of debris flow sediments in CJB indicates that the limestone proportion is larger than that of phyllites (Fig. 11). This suggests that many of the clasts may come from the upper limestone hillslopes, though the lower phyllite hillslopes that stored some limestone gravels may also contribute to the debris flows. The debris flows may be associated with heavy rainfall events that caused landsliding of the hillside regolith or colluvium in the headwater valleys. Because the hillslope gradient is generally greater than 40°, which is close to the repose angle of coarse blocky materials (Beakawi Al-Hashemi and Baghabra Al-Amoudi, 2018), the hillslope regolith are prone to initiation due to the increase of pore water pressures during heavy rainfalls (Iverson, 1997; Papa et al., 2013; Takahashi, 2009; Tang et al., 2011). Both intense rainfall events and sediment supply are constraining factors for the occurrence of debris flows. The variations of temperature (affects snowmelt activity), vegetation cover as well as the activity of the strike-slip thrust may all affect the supply of loose sediment from the limestone hillslopes.

The mudflow sediments are mainly composed of yellowish fine materials (accounting for ~65% in weight), suggesting that most materials comprising the mudflows came from the loess-covered hillslopes. The Fm’ sediments contain limestones and phyllites (Fig. 11). The phyllite gravels may reflect the contribution of phyllite regolith underlying loess, and the limestone gravels may come from the upstream limestone hillslopes, from the phyllite hillslopes that stored limestone gravels or from the collapse of the $F2^*$ alluvial fans. The formation of mudflows is usually associated with intense or prolonged rainfall events that cause loess landslides and large runoffs (Ma et al., 2005; Wu et al., 2016; Xu et al., 2012b; Zhang et al., 2019). Many loess landslides develop on the loess-covered hillslopes in the CJB valley (Fig. 4), and landslide deposits are generally found in the main channels. Upon intense rainfall events, these materials (both the loess that cover the hillslopes and that stored in the main channels) may be weakened by channel erosion and underground water seepage leading to loess collapse or landslides, which may be transformed into mudflows by runoff. Specifically, we infer that landslide development may be the major mechanism for the evolution of the loess-covered phyllite hillslopes. According to our field investigation, the channels are shallow and gentle in the upper part of the phyllite hillslopes, probably indicating little incision into the ground (Fig. 12a). However, the channels deepen further downstream and incise into the phyllite bedrocks (Fig. 12b). The channels are choked either by limestone boulders (Fig. 12c) or loess landslides (Figs. 12d&12e), forming water jumps of up to 5 m deep. Sink holes with a visible depth of about 3 m are distributed along the loess hillslopes (Fig. 12f). It is obvious that the valley floors are steeper in the lower phyllite hillslopes than those in the upper phyllite hillslopes. These morphological characteristics drive us to propose the following hillslope evolution stages:

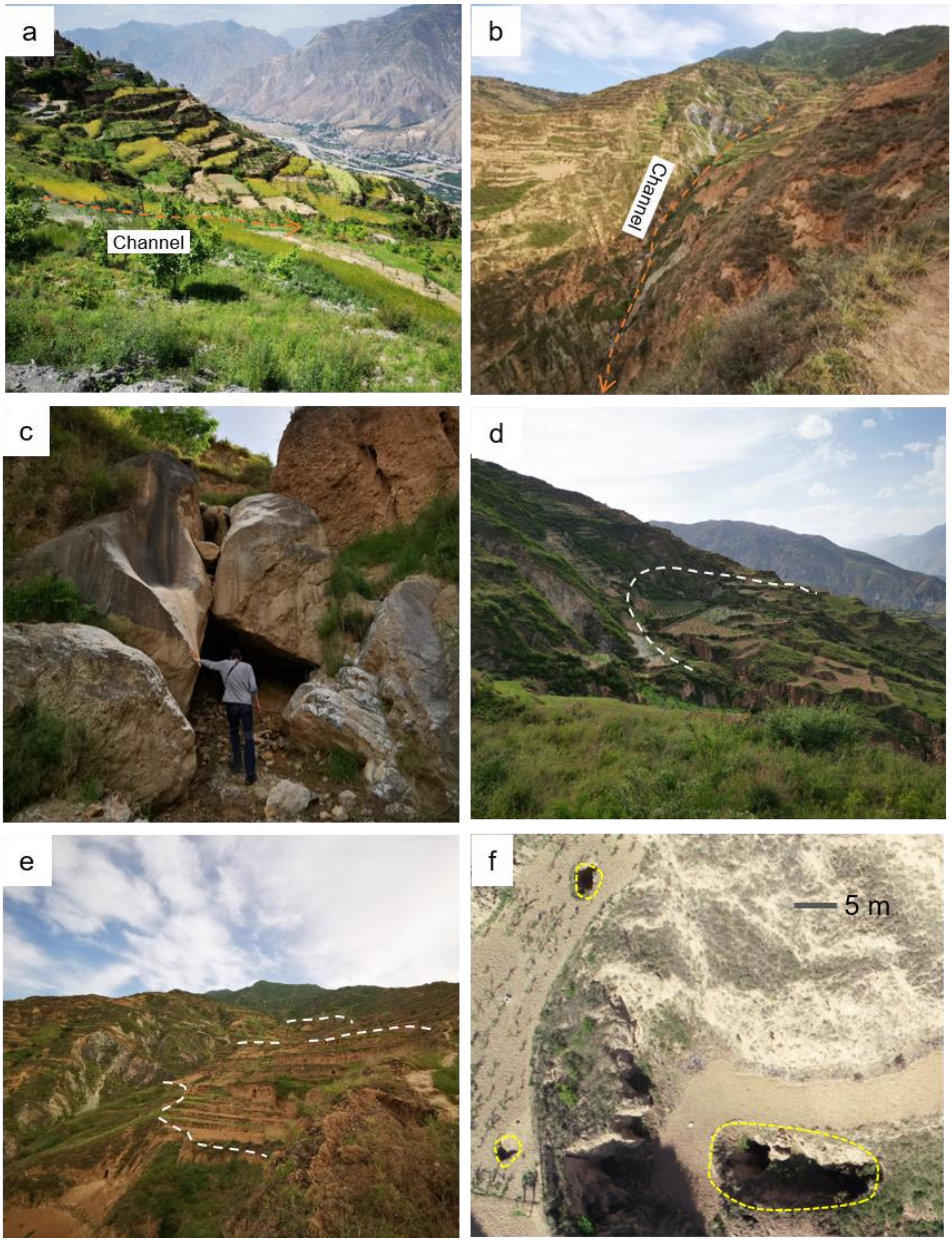

Fig. 12. Characteristics of the loess-covered phyllite hillslopes. a. The relatively smooth and shallow channels in the upper section of the phyllite hillslope; b. The steep channels in the lower section of the hillslope; c. Large boulders choking the channels; d & e. Landslides developed on the hillslopes. f. Sink holes developed on the surface of hillslopes.

Stage 1: The incision of the Bailong River formed the steep hillslopes and the wide river valley, providing the accommodation space and steepness to initiate landslides. The F2* and F4 alluvial fans developed on the base of a river terrace level that is ~100 m above the modern river (Fig. 6). This high-level terrace indicates the incision depth of the Bailong River, and it is likely that this incision event initiated the hillslope processes that formed the lower-level alluvial fans in both valleys.

Stage 2: Some relatively small landslides developed along the edges of the phyllite hillslopes or river terraces (Fig. 13, Stage 2). These landslides probably represent the initial stage of valley development. Many sink holes were discovered on the loess hillslopes during our field investigation (Fig. 13), and these sink holes may become the preferential pathways for water infiltration that weaken the hillslope base and lead to landslides (Xu et al., 2012a; Zeng et al., 2016)

Stage 3: Once landslides occurred, new failures are prone to occur along the head scarps due to water seepage (Qi et al., 2018; Xu et al., 2012b; Zeng et al., 2016). Consequently, landslides recurred along the newly-formed scarps and erode the upper hillslopes retrogressively, forming prolonged gullies (Fig. 13, Stage 3).

Stage 4: The prolonged gullies evoke higher absolute water discharges due to the enlargement of the watershed area. The sediment discharges may also increase but may be lower than the water discharges because sediment entrainment by surface runoff is far less efficient than landsliding. Moreover, the process of surface erosion may be impeded by enhanced vegetation cover during wet climates. Consequently, gully incision is initiated, and the deeply-incised gullies may activate the side-hillslopes, leading to landslides moving almost perpendicular to the gully (Fig. 13, Stage 4). This loop of landslide-gully formation and incision-landslide forms a positive feedback and is probably the major reason for the valley evolution of the study area.

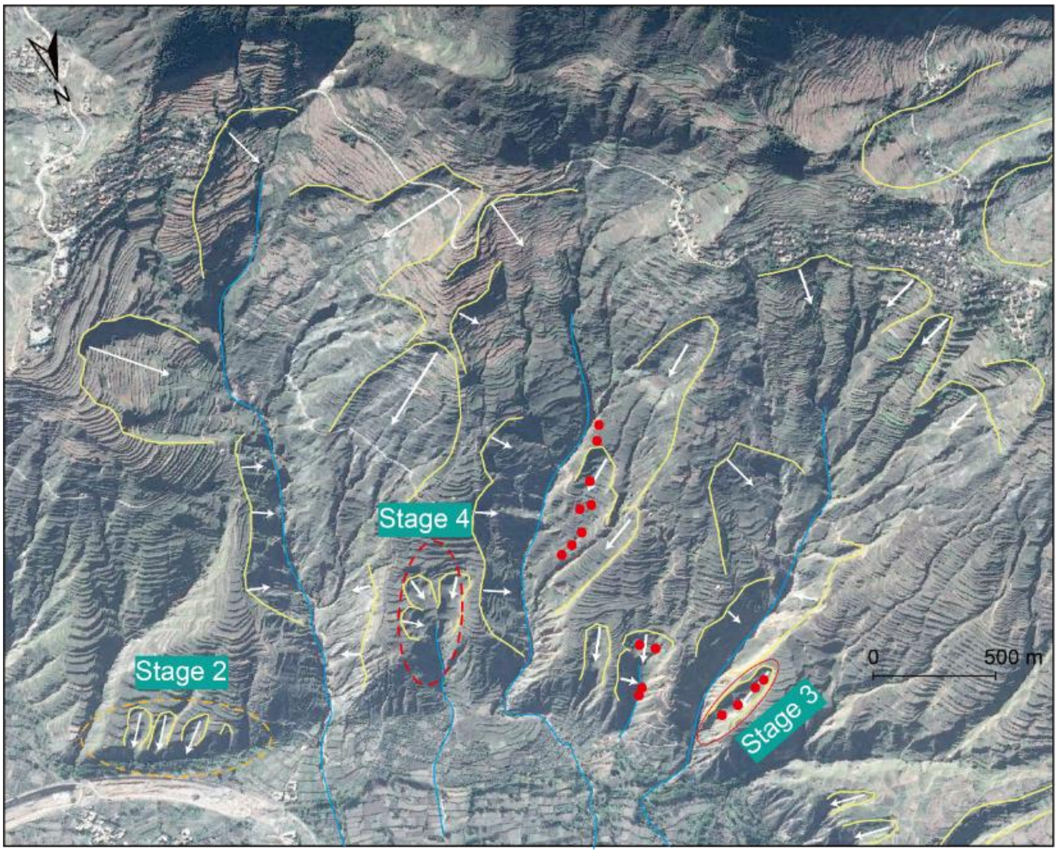

Fig. 13. Landslide distribution in the study area. Blue lines are the main streams developed in the corresponding valley. Yellow lines are the head scarps of landslides and white arrows show the sliding direction. Red dots are sink holes that we discovered along the hillslopes. Stages 2, 3, and 4 are the inferred valley evolution stages illustrated in the main content.

5.2. Timing of fan aggradation and incision and controlling factors

The seven radiocarbon dated samples provide ^{14}C ages between c. 10.1 – 4.9 kyr BP. As the base of the alluvial fan was not uncovered, we do not know the beginning time of fan aggradation. It is possible that fan formation started with the formation of the wide-flood plain/terraces by the Bailong River, such that accommodation space is created for sediments to accumulate. Two samples (samples 02 and 06) were taken from the upper parts of the fan exposures. Sample 02, taken from a proximal fan exposure, provides an age of 5.96 ± 0.04 kyr BP; sample 06, taken from a distal fan exposure away from the main channel, provides an age of 4.92 ± 0.04 kyr BP. Provided that the ages are broadly accurate, the aggradation period is confined between c. 10.1 and 4.9 kyr BP, and the incision period occurred shortly after 4.9 kyr BP, forming the present channel. However, as these ages may be contaminated by older organic materials from hillslopes, it is likely that the periods of aggradation and incision occur prior to the aforementioned time ranges. Whatever the condition is, it can be ascertained that the timing of fan incision and aggradation in the CJB valley is younger than that in the GLP valley. In the GLP valley, most of the samples taken from the lower and middle section of the F3 alluvial fans provide OSL ages between 21.7 -13.3 ka (Li et al., 2018), and the samples taken from the top of the alluvial fans provide ages between 7.1-8.5 ka. Since 7 ka, gross fan aggradation terminated, and fan incision started, which finally formed the deeply incised F3 exposures. Both the aggradation and the incision periods in the CJB valley occur later than the respective periods in the GLP valley.

The timing of aggradation and incision in GLP and CJB are plotted against the climatic records of East Asia Summer Monsoon in Fig. 14. In the GLP valley, fan aggradation occurred both in the cold-dry glacial period and the increasingly warm-wet early Holocene (Fig. 14), while fan incision occurred in the mid-Holocene when the climate was warmest and wettest (An et al., 2003; Feng et al., 2006; Zhao et al., 2009; Wang et al., 2014; Chen et al., 2015). In a previous paper (Li et al., 2018), we suggested that the fan aggradation may be associated with surplus sediment supply caused by enhanced frost shattering and decreased vegetation cover during the cold and dry LGM and probably the early Holocene, while incision was caused by a decrease in sediment supply due to vegetation recovery and an increase in the frequency of flood discharges in the warm-wet mid-Holocene.

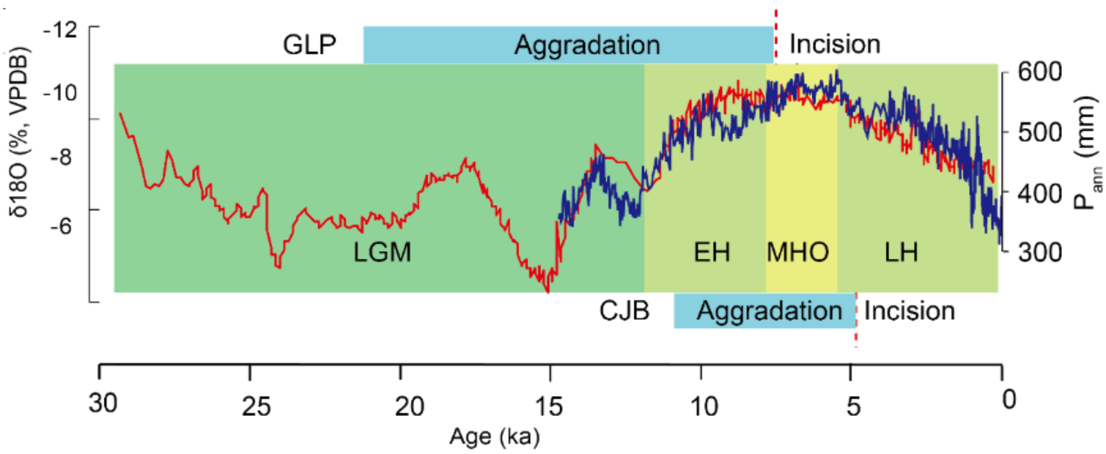

Fig. 14. Regional climatic records and timing of fan incision in the GLP and the CJB valleys. The red curve is the Sanbao Cave $\delta^{18}O$ speleothem record (Wang et al., 2008), while the blue curve is a pollen-based precipitation record from Gonghai Lake (Chen et al., 2015). LGM=last

glacial maximum, EH=early Holocene, MHO=mid-Holocene maximum, and LH=late Holocene.

In contrast, the fan aggradation in CJB occurred in the early and mid-Holocene corresponding to an increasingly wet and warm condition. Provided that our ^{14}C ages are right, the fan aggradation in this period may be related to the increased frequencies of heavy rainfall events that enhanced the frequencies of mudflow/debris flow events. Studies of palaeo-mudflow sediments in nearby areas (e.g., Zha et al., 2019; Yin et al., 2014) have shown the trend of enhanced activities of mudflows in wet climates. Moreover, recent heavy rainfall events that caused wide-spread distributions of mudflows in nearby areas also support the positive relationship between mudflows and strong rainfall events. For example, heavy rainfall with a total of 93.4-369 mm falling in 16 hours in Tianshui on 2013-05-14 initiated numerous shallow loess landslides which were transformed into mudflows/debris flows (Guo et al., 2018). For the CJB valley, heavy rainfall during periods of wettter climate may initiate landsliding of the regolith/loess-covered hillslopes, which may be transformed into debris flows/mudflows by runoff, forming fan aggradation. In contrast, due to comparatively low loess cover, the GLP valley may produce relatively higher water discharges than sediment supply during the wet climate, which would promote incision. The areal distribution of loess only accounts for 9% of the GLP area (Table 1), meaning that loess landslides may not be the dominant processes in GLP. Most solid materials may come from landsliding or surface erosion of hillslope regolith, the production of which may be impeded by the recovered vegetation during the wet climate. Consequently, more water discharge is produced relative to sediment supply, leading to fan incision.

Assuming the 14C ages are correct, incision in CJB occurred after c. 4.9 kyr BP, though we do not know the precise timing of fan incision in CJB. Nevertheless, we can broadly determine that the fan incision occurred in the Late Holocene. We infer that both intrinsic and extrinsic mechanisms may contribute to the fan incision. For intrinsic mechanisms, the aggradation of the alluvial fan may increase the fan surface gradients, and fan incision may be initiated when the surface gradients approach the intrinsic geomorphic threshold (Harvey, 1984; Schumm et al., 1987; Bowman, 2019). Besides, the expansion of the alluvial fan may decrease the aggradation rate of the alluvial fan provided that the external conditions controlling sediment/water ratios remain stable (Clarke et al., 2010). This decreasing aggradation rate may cause sheetflow-dominated conditions transformed into channelized flows, leading to initiation of fan incision (Nicholas et al., 2009; Clarke et al., 2010).

The extrinsic mechanisms may include the change of base level and climate, while the effect of tectonism is unlikely to be an influence at this time scale. As the Bailong River is the base-level for the alluvial fans in this tributary-junction setting, variation in the Bailong River may have been a factor affecting the fan incision in CJB. Both lateral erosion and vertical incision of the Bailong River may cause fan incision starting from fan margins back towards the fan head (Harvey, 2012). However, according to our field investigations, distally-induced failures along the fan margins only form localized gullies confined to within several meters back into the fan surfaces. Therefore, base-level change may provide little influence on the fan incision in CJB, though the steep distal fan edges may have been related to the lateral-erosion by the Bailong River.

Instead the fan incision in CJB may have been mainly caused by proximally-induced fan-head trenching. A channel that flows out of a feeder catchment and pinches out to the fan margin (Fig. 13: the channel flowing out from the stage 4 valley) may suggest that proximally induced fan-head trenching is the primary regime for hillslope-river coupling in CJB. Fan-head trenching is most likely triggered by critical power relationships that are governed by the balance between flood discharges and sediment supply (Bull, 1979; Harvey, 2002; 2012). Climate has been regarded as a primary factor controlling critical power relationships (Harvey, 2012). For the study area, the Late Holocene was likely characterized by a gross trend towards increased drying (Fig. 14). Pollen records from the nearby western part of the Chinese Loess Plateau (An et al., 2003; Feng et al., 2006) suggest that vegetation cover changed from an ulmus-dominated forest-steppe (4.9- 4.0 kyrs BP) to a steppe (4.0 – 3.1 kyrs BP), and further to a desert-steppe (3.1 – 2.9 kyrs BP). Generally, dry conditions should provoke aggradation rather than incision, but even in average dry conditions it is the frequency and the intensity of precipitation events that are most effective in driving geomorphic work (Blair and McPherson, 1994; Owen et al., 2014). During periods of dry climate, the magnitude and frequency of individual precipitation events may decrease. Specifically, when the magnitudes of individual precipitation events drop below the threshold for landslide initiation, landslides may not then active geomorphic processes. Consequently, the amount of sediment supply may decrease substantially and become relatively reduced in comparison to water discharge, causing fan incision. In contrast, the F2 alluvial fans of GLP valley formed in the Late Holocene (Li et al., 2018). We infer that the formation of the F2 alluvial fans was a result of the continued incision of the F3 alluvial fans. The storm events during this period may have eroded the materials of the F3 alluvial fans and deposited them on the floodplains of the Bailong River, while during the previous incision period in the mid-Holocene, sediments were transported by the higher runoff discharges into the Bailong River, causing net incision.

Interestingly, the fan formation period constrained by our ^{14}C ages in CJB is consistent with the study of Chen et al. (2008) who focused on an alluvial fan on the southeastern margin of the Tibetan Plateau (Table 4). Their OSL ages constrained the fan aggradation period between 10.6 – 4.5 ka corresponding to a strengthened Asian Summer Monson. Wang et al. (2000) also produced three ^{14}C ages ranging between 7340 – 6410 yrs BP from three different alluvial fans (including one ^{14}C age for the CJB fan) that are at relatively the same height above the Bailong River (Table 4). These three ages may partially suggest the timing of fan aggradation and coincides with the aggradation period defined in this study. From these pieces of evidence, we hypothesise that a common fan-formation period likely existed for small-sized tributaries on the eastern margin of the Tibetan Plateau, and that this period was associated with warm-wet climatic conditions. It is tempting to infer that alluvial fans from small-sized valleys may have a common climatic control, with fan aggradation occurring during warm-wet climatic conditions, while in contrast fan incision occurred during relatively dry-cold conditions. It is noteworthy that the colder conditions during the Late Holocene would have been much less intense than the cold conditions at the end of the last glaciation. This proposed climatic control for alluvial fans of small-sized valleys is the opposite to that proposed for the alluvial fans of mid-sized valleys (Li et al., 2018) where fan aggradation corresponds to the cold-dry conditions in the last glacial maximum while fan incision corresponds to the warm-wet conditions in the mid-Holocene. These two distinct climate-fan response regimes may be attributed to the different capacities in producing runoffs for small- and mid-sized valleys: the mid-sized valley may produce larger runoff discharges than the small-sized valley corresponding to the same rainfall events. The variation of loess distribution, which determines the primary processes for fan formation in the two valleys, may also be a factor. Again, as the ^{14}C ages reported in this study may be contaminated by older hillslope materials, this hypothesis cannot be validated through this study. More research on similar types of alluvial fans and cross-validation of different dating methods are needed.

Table 4 Characteristics for other alluvial fans studied on the Eastern Tibetan Plateau. A is catchment area; H is the height of the alluvial fan surface above the river. CP represents constructing processes for alluvial fans. DF refers to debris flows, while MF refers to mudflows.

Research	Location	A (km^2)	H(m)	CP	Dating method	Time
Wang et al (2000)	Luba (Fig. 2)	5.5	5	DF	^{14}C	6410 yr BP
	CJB (Fig. 2)	1.1	8	DF&MF	^{14}C	7340 yr BP
	Tiebuqu (unknown)	--	8	DF	^{14}C	6810 yr BP
Chen et al (2008)	Waka (N 28.24° E 99.32°)	8.5	6	DF	OSL	10.6-4.5 ka

6. Conclusion

This paper studies the evolution of the alluvial fans from a small-sized tributary valley along the Bailong River. Specifically, we focus on the nature of the fan-forming process and the timing of fan aggradation and incision. Sedimentary logging and lithofacies analyses for seven fan exposures allow us to identify the primary fan forming processes: debris flows and mudflows. Specifically, we infer that the materials of mudflows may be associated with the occurrence of landslides on the loess-covered phyllite hillslopes, while the sediments from debris flows may be attributed to the rock falls or regolith from the limestone hillslopes. Humin fractions were extracted from the paleosols that were developed in mudflow sediments for ^{14}C dating. The acid-alkaline-acid treatment for soil samples removed the potential contamination by younger organic materials, however, the clay-sized humin fraction may be legacies of hillslope materials. Consequently, the ^{14}C ages reported in this study may provide older ages than the true deposition time of the mudflow sediments, but this remains untested at present.

Our seven ^{14}C ages constrain the fan formation period to between 10.1 - 4.9 kyr BP, with fan incision occurring after 4.9 kyr BP in CJB. At this stage we cannot rule out that fan formation and incision in CJB may be more recent than dated using the bulk organic matter 14C dating. However, in any case the times of fan aggradation and incision in CJB are younger than those in the GLP valley.

If the 14C ages are taken as broadly reliable, the fan aggradation period was associated with a gradually strengthened Asian Summer Monsoon, featuring a warm-wet climate. The increased magnitude and frequency of individual rainfall events that increased the activities of landslides may have been the reason for fan aggradation in CJB. In contrast, the incision period was associated with a weakened Asian Summer Monsoon and a drying climate. The intrinsic factors behind this may be related to the oversteepening on the fan surface and the decreasing aggradation rate associated with fan expansion. The extrinsic factor of base-level change was precluded because our analyses indicate a proximally-induced fan incision regime. However, the impact of the extrinsic factor of climate may be associated with decreased magnitude of heavy rainfalls and would have thus impeded activities of loess landslides in the dry climate.

The fan aggradation period defined by the ^{14}C ages is consistent with an alluvial fan of similar thickness in the southeastern Tibetan Plateau and two other fans along the Bailong River. Therefore, we propose that a seemingly consistent climatic control on the evolution of alluvial fans sourced from small-sized tributary valleys along the Tibetan plateau margin is emerging. However, more research on cross-validation of the numerical ages is required to test this.

Acknowledgments

We thank the reviewers for their constructive comments that have improved the quality of the paper. This research was supported by National Key Research and Development Program of China (Grant No 2017YFC1501005), the “Postdoctoral International Exchange Program in Lanzhou, China”, the National

Natural Science Foundation of China (Grant No. 41907224), the Key Technology Research and Development Program of the Ministry of Gansu Province, China (Grant No. 19ZD2FA002), the Program for International S&T Cooperation Projects of Gansu Province (No. 2018-0204-GJC-0043), and the Fundamental Research Funds for the Central Universities (Grant Nos. lzujbky-2020-pd12; lzujbky-2019-28; lzujbky-2020-sp03).

References

An, C., Feng, Z., Tang, L., 2003. Evidence of a humid mid-Holocene in the western part of Chinese Loess Plateau. Chinese Science Bulletin 48, 2472-2479.

Bagnold, R.A., 1954. Experiments on a gravity-free dispersion of large solid spheres in a Newtonian fluid under shear, Proceedings of the Royal Society of London A: Mathematical, Physical and Engineering Sciences. The Royal Society, pp. 49-63.

Beakawi Al-Hashemi, H.M., Baghabra Al-Amoudi, O.S., 2018. A review on the angle of repose of granular materials. Powder Technology 330, 397-417.

Blair, T.C., Mcpherson, J.G., 1994. Alluvial fan processes and forms, Geomorphology of desert environments. Springer, pp. 354-402.

Bridgland, D.R., Westaway, R., 2014. Quaternary fluvial archives and landscape evolution: a global synthesis. Proceedings of the Geologists' Association 125, 600-629.

Bronk Ramsey, C. (2009). Bayesian Analysis of Radiocarbon Dates. Radiocarbon, 51(1), 337-360. doi:10.1017/S0033822200033865.

Cabré, A., Aguilar, G., Mather, A.E., Fredes, V., Riquelme, R., Tributary-junction alluvial fan response to an ENSO rainfall event in the El Huasco watershed, northern Chile. doi:10.1177/0309133319898994.

Chen, F., Xu, Q., Chen, J., Birks, H.J.B., Liu, J., Zhang, S., Jin, L., An, C., Telford, R.J., Cao, X., 2015. East Asian summer monsoon precipitation variability since the last deglaciation. Scientific reports 5, 11186.

Chen, J., Dai, F., Yao, X., 2008. Holocene debris-flow deposits and their implications on the climate in the upper Jinsha River valley, China. Geomorphology 93, 493-500.

Cheng, B., Liu, J., Chen, S., Zhang, Z., Shen, Z., Yan, X., Li, F., Chen, G., Zhang, X., Wang, X., Chen, J., 2020. Impact of Abrupt Late Holocene Monsoon Climate Change on the Status of an Alpine Lake in North China. Journal of Geophysical Research: Atmospheres, 125, e2019JD031877.

Clarke, L., Quine, T.A., Nicholas, A., 2010. An experimental investigation of autogenic behaviour during alluvial fan evolution. Geomorphology 115, 278-285.

Coulthard, T., Lewin, J., Macklin, M., 2005. Modelling differential catchment response to environmental change. Geomorphology 69, 222-241.

Crosta, G.B., Frattini, P., 2004. Controls on modern alluvial fan processes in the central Alps, northern Italy. Earth Surface Processes and Landforms 29, 267-293.

Curry, R.R., 1966. Observation of alpine mudflows in the Tenmile Range, central Colorado. Geological Society of America Bulletin 77, 771-776.

Dasgupta, P., Manna, P., 2011. Geometrical mechanism of inverse grading in grain-flow deposits: An experimental revelation. Earth-Science Reviews 104, 186-198.

de Scally, F.A., Owens, I.F., Louis, J., 2010. Controls on fan depositional processes in the schist ranges of the Southern Alps, New Zealand, and implications for debris-flow hazard assessment. Geomorphology 122, 99-116.

Feng, Z.-D., Tang, L., Wang, H., Ma, Y., Liu, K.-b., 2006. Holocene vegetation variations and the associated environmental changes in the western part of the Chinese Loess Plateau. Palaeogeography, Palaeoclimatology, Palaeoecology 241, 440-456.

Geach, M.R., Viveen, W., Mather, A.E., Telfer, M.W., Fletcher, W.J., Stokes, M., Peyron, O., 2015. An integrated field and numerical modelling study of controls on Late Quaternary fluvial landscape development (Tabernas, southeast Spain). Earth Surface Processes and Landforms 40, 1907-1926.

Guo, F. Y., Meng, X. M., Li, Z. H., Xie, Z. T., Chen, G., He, Y. F., 2015. Characteristics and causes of assembled geo-hazards induced by the rainstorm on 25th July 2013 in Tianshui City, Gansu, China. Mountain Research, 33 (1), 100-107 (in Chinese).

Harvey, A., 1996. The role of alluvial fans in the mountain fluvial systems of southeast Spain: implications of climatic change. Earth Surface Processes and

Landforms 21, 543-553.

Harvey, A.M., 2012. The coupling status of alluvial fans and debris cones: a review and synthesis. Earth Surface Processes and Landforms 37, 64-76.

Harvey, A.M., Stokes, M., Mather, A., Whitfield, E., 2016. Spatial characteristics of the Pliocene to modern alluvial fan successions in the uplifted sedimentary basins of Almería, SE Spain: review and regional synthesis. Geological Society, London, Special Publications 440, SP440. 445.

Hungr, O., Evans, S., Bovis, M., Hutchinson, J., 2001. A review of the classification of landslides of the flow type. Environmental & Engineering Geoscience 7, 221-238.

Hungr, O., Leroueil, S., Picarelli, L., 2014. The Varnes classification of landslide types, an update. Landslides 11, 167-194.

Inoue, Y., Hiradate, S., Sase, T., Hosono, M., Morita, S., Matsuzaki, H., 2011. Using ^{14}C dating of stable humin fractions to assess upbuilding pedogenesis of a buried Holocene humic soil horizon, Towada volcano, Japan. Geoderma 167-168, 85-90.

Iverson, R.M., 1997. The physics of debris flows. Reviews of geophysics 35, 245-296.

Kar, R., Chakraborty, T., Chakraborty, C., Ghosh, P., Tyagi, A.K., Singhvi, A.K., 2014. Morpho-sedimentary characteristics of the Quaternary Matiali fan and associated river terraces, Jalpaiguri, India: Implications for climatic controls. Geomorphology 227, 137-152.

Khan, M.A., Haneef, M., Khan, A.S., Tahirkheli, T., 2013. Debris-flow hazards on tributary junction fans, Chitral, Hindu Kush Range, northern Pakistan. Journal of Asian Earth Sciences 62, 720-733.

Li, Y., Armitage, S.J., Stevens, T., Meng, X., 2018. Alluvial fan aggradation/incision history of the eastern Tibetan plateau margin and implications for debris flow/debris-charged flood hazard. Geomorphology 318, 203-216.

Ma, D.T., Cui, P., Zhang, J.S., L, H.L., 2005. Formation causes and features of mudflows in the Loess Plateau, China. Arid Land Geography 28, 435-440 (In Chinese).

Mather, A., Stokes, M., Whitfield, E., 2017. River terraces and alluvial fans: The case for an integrated Quaternary fluvial archive. Quaternary Science Reviews 166, 74-90.

Mather, A.E., Stokes, M., 2018. Bedrock structural control on catchment-scale connectivity and alluvial fan processes, High Atlas Mountains, Morocco. 440, 103-128.

Miall, A.D., 2006. The geology of fluvial deposits: sedimentary facies, basin analysis, and petroleum geology. Springer.

Middleton, G.V., 1970. Experimental studies related to problems of flysch sedimentation, in Lajoie, J., ed., Flysch Sedimentatology in North America: Geol. Assoc. Canada Special Paper 7, p 253-272.

Nicholas, A., Clarke, L., Quine, T., 2009. A numerical modelling and experimental study of flow width dynamics on alluvial fans. Earth Surface Processes and Landforms 34, 1985-1993.

Nicholas, A.P., Quine, T.A., 2007. Modeling alluvial landform change in the absence of external environmental forcing. Geology 35, 527-530.

Owen, L., Windley, B., Cunningham, W., Badamgarov, J., Dorjnamjaa, D., 1997. Quaternary alluvial fans in the Gobi of southern Mongolia: evidence for neotectonics and climate change. Journal of Quaternary Science 12, 239-252.

Owen, L.A., Clemmens, S.J., Finkel, R.C., Gray, H., 2014. Late Quaternary alluvial fans at the eastern end of the San Bernardino Mountains, Southern California. Quaternary Science Reviews 87, 114-134.

Papa, M., Medina, V., Ciervo, F., Bateman, A., 2013. Derivation of critical rainfall thresholds for shallow landslides as a tool for debris flow early warning systems. Hydrology and Earth System Sciences 17, 4095-4107.

Pessenda, L.R., Gouveia, S.M., Aravena, R., 2001. Radiocarbon dating of total soil organic matter and humin fraction and its comparison with ^{14}C ages of fossil charcoal. doi: DOI: 10.1017/S0033822200041242.

Pierson, T.C., Costa, J.E., 1987. A rheologic classification of subaerial sediment-water flows. Reviews in engineering geology 7, 1-12.

Qi, X., Xu, Q., Liu, F., 2018. Analysis of retrogressive loess flowslides in Heifangtai, China. Engineering Geology 236, 119-128.

Qian, N., Wang, Z. H., 1983. Sediment movement mechanics. Science Publication: Beijing (in Chinese).

Reimer PJ, Bard E, Bayliss A et al (2013) IntCal13 and Marine13 radiocarbon age calibration curves, 0–50,000 years cal BP. Radiocarbon 55:1,869–1,887.

Ritter, J.B., Miller, J.R., Enzel, Y., Wells, S.G., 1995. Reconciling the roles of tectonism and climate in Quaternary alluvial fan evolution. Geology 23, 245-248.

Santangelo, N., Daunis‐i‐Estadella, J., Di Crescenzo, G., Di Donato, V., Faillace, P., Martín‐Fernández, J., Romano, P., Santo, A., Scorpio, V., 2012. Topographic predictors of susceptibility to alluvial fan flooding, Southern Apennines. Earth Surface Processes and Landforms 37, 803-817.

Schumm, S. A., Mosley, M. P, Weaver, W. E., 1987. Experimental fluvial geomorphology. Wiley: Chichester.

Singh, A.K., Jaiswal, M.K., Pattanaik, J.K., Dev, M., 2016. Luminescence chronology of alluvial fan in North Bengal, India: Implications to tectonics and climate. Geochronometria 43, 102-112.

Sohn, Y., 1997. On traction-carpet sedimentation. Journal of Sedimentary Research 67, 502-509.

Spelz, R.M., Fletcher, J.M., Owen, L.A., Caffee, M.W., 2008. Quaternary alluvial-fan development, climate and morphologic dating of fault scarps in Laguna Salada, Baja California, Mexico. Geomorphology 102, 578-594.

Stokes, M., Cunha, P.P., Martins, A.A., 2012. Techniques for analysing Late Cenozoic river terrace sequences. Geomorphology 165-166, 1-6.

Stokes, M., Mather, A.E., 2015. Controls on modern tributary-junction alluvial fan occurrence and morphology: High Atlas Mountains, Morocco. Geomorphology 248, 344-362.

Stolle, A., Langer, M., Blöthe, J.H., Korup, O., 2015. On predicting debris flows in arid mountain belts. Global and Planetary Change 126, 1-13.

Suresh, N., Bagati, T.N., Kumar, R., Thakur, V.C., 2007. Evolution of Quaternary alluvial fans and terraces in the intramontane Pinjaur Dun, Sub-Himalaya, NW India: Interaction between tectonics and climate change. Sedimentology 54, 809-833.

Takahashi, T., 1981. Debris flow. Annual review of fluid mechanics 13, 57-77.

Takahashi, T., 2009. A review of Japanese debris flow research. International Journal of Erosion Control Engineering 2, 1-14.

Tang, C., Rengers, N., van Asch, T.W., Yang, Y., Wang, G., Luino, F., 2011. Triggering conditions and depositional characteristics of a disastrous debris flow event in Zhouqu city, Gansu Province, northwestern China. Natural Hazards & Earth System Sciences 11, 2903-2912.

Viseras, C., Calvache, M.a.L., Soria, J.M., Fernández, J., 2003. Differential features of alluvial fans controlled by tectonic or eustatic accommodation space. Examples from the Betic Cordillera, Spain. Geomorphology 50, 181-202.

Wang, H., Chen, J., Zhang, X., Chen, F., 2014. Palaeosol development in the Chinese Loess Plateau as an indicator of the strength of the East Asian summer monsoon: Evidence for a mid-Holocene maximum. Quaternary International 334, 155-164.

Wang, J., Wang, Y., Shi, Y., 2000. A preliminary study on debris flow and environmental evolution in Holocene at the Bailongjiang River Valley. Journal of Southwest China Normal University (Natural Science) 25, 452-456 (In Chinese).

Wang, Y., Cheng, H., Edwards, R.L., Kong, X., Shao, X., Chen, S., Wu, J., Jiang, X., Wang, X., An, Z., 2008. Millennial-and orbital-scale changes in the East Asian monsoon over the past 224,000 years. Nature 451, 1090-1093.

Welsh, A., Davies, T., 2011. Identification of alluvial fans susceptible to debris-flow hazards. Landslides 8, 183-194.

Went, D.J., 2005. Pre‐vegetation alluvial fan facies and processes: an example from the Cambro‐Ordovician Rozel Conglomerate Formation, Jersey, Channel Islands. Sedimentology 52, 693-713.

Wu, Z., Zhiqiang, Y., Qiang, X., Xiaoguang, Q., 2016. Formation Mechanisms and Geomorphic Evolution of the Erlian Mudflow Fans, Eastern Guide Basin of the Upper Reaches of Yellow River. Acta Geologica Sinca 90, 578-589.

Xiong, H., Cui, Z. J., 1991. Discussion on sedimentary environment and debris flow deposits. Mountain Research, 9 (1): 7-13 (in Chinese).

Xiong, M., Meng, X., Wang, S., Guo, P., Li, Y., Chen, G., Qing, F., Cui, Z., Zhao, Y., 2016. Effectiveness of debris flow mitigation strategies in mountainous regions. Progress in Physical Geography, 0309133316655304.

Xu, L., Dai, F.C., Tham, L.G., Zhou, Y.F., Wu, C.X., 2012a. Investigating landslide-related cracks along the edge of two loess platforms in northwest

China. Earth Surface Processes and Landforms 37, 1023-1033.
Xu, L., Qiao, X., Wu, C., Iqbal, J., Dai, F., 2012b. Causes of landslide recurrence in a loess platform with respect to hydrological processes. Natural Hazards 64, 1657-1670.
Zeng, R.Q., Meng, X.M., Zhang, F.Y., Wang, S.Y., Cui, Z.J., Zhang, M.S., Zhang, Y., Chen, G., 2016. Characterizing hydrological processes on loess slopes using electrical resistivity tomography – A case study of the Heifangtai Terrace, Northwest China. Journal of Hydrology 541, 742-753.
Zha, X., Huang, C., Pang, J., Li, Y., Liu, J., Cuan, Y., Wang, N., 2019. Sedimentary records of holocene palaeo-mudflow events in Tianshui basin of the western Loess Plateau, China. Quaternary International 521, 129-137.
Zhang, F., Yan, B., Feng, X., Lan, H., Kang, C., Lin, X., Zhu, X., Ma, W., 2019. A rapid loess mudflow triggered by the check dam failure in a bulldoze mountain area, Lanzhou, China. Landslides 16, 1981-1992.
Zhao, Y., Yu, Z., Chen, F., Zhang, J., Yang, B., 2009. Vegetation response to Holocene climate change in monsoon-influenced region of China. Earth-Science Reviews 97, 242-256.